Lung Cancer 159 (2021) 34–41

Contents lists available at ScienceDirect

Lung Cancer

journal homepage: www.elsevier.com/locate/lungcan

The Pandora's box of novel technologies that may revolutionize lung cancer

Habib Sadeghi Rad [a,b], Hamid Sadeghi Rad [c], Yavar Shiravand [d], Payar Radfar [e], David Arpon [b,f], Majid Ebrahimi Warkiani [e], Ken O'Byrne [a,b,f], Arutha Kulasinghe [a,b,f,*]

[a] Queensland University of Technology, Centre for Genomics and Personalised Health, Cancer and Ageing Research Program, School of Biomedical Sciences, Faculty of Health, Woolloongabba, QLD, Australia
[b] Translational Research Institute, Woolloongabba, QLD, Australia
[c] School of Medicine, Golestan University of Medical Sciences, Golestan, Iran
[d] Department of Molecular Medicine and Medical Biotechnology, University of Naples Federico II, Naples, Italy
[e] University of Technology Sydney, Sydney, NSW, Australia
[f] Princess Alexandra Hospital, Woolloongabba, QLD, Australia

ARTICLE INFO

Keywords:
Lung cancer
Spatial transcriptomics
Multiplex immunohistochemistry
Molecular barcoding
Tumour microenvironment

ABSTRACT

Non-small cell lung cancer (NSCLC) is one of the most common cancers globally and has a 5-year survival rate ~20%. Immunotherapies have demonstrated long-term and durable responses in NSCLC patients, although they appear to be effective in only a subset of patients. A more comprehensive understanding of the underlying tumour biology may contribute to identifying those patients likely to achieve optimal outcomes. Profiling the tumour microenvironment (TME) has shown to be beneficial in addressing fundamental tumour-immune cell interactions. Advances in multiplexing immunohistochemistry and molecular barcoding has led to recent advances in profiling genes and proteins in NSCLC. Here, we review the recent advancements in spatial profiling technologies for the analysis of NSCLC tissue samples to gain new insights and therapeutic options for NSCLC. The combination of spatial transcriptomics combined with advanced imaging is likely to lead to deep insights into NSCLC tissue biology, which can be a powerful tool to predict likelihood of response to therapy.

1. Introduction

1.1. Lung cancer

Lung cancer is the leading cause of cancer death in the United States, and globally [1]. Small cell lung cancer (SCLC) and non-small cell lung cancer (NSCLC) are the two main histological subtypes of lung cancer, with NSCLC accounting for 76% of all cases [2]. Advances in genomic profiling have defined the pattern of classification in which lung cancers are characterized. Tumour mutations, rearrangements, and gene expression profiles may be targeted with specific agents or immune checkpoint inhibitors (ICIs) [3–5]. ICIs have expanded the therapeutic options for NSCLC in the past ten years. However, only a subset of patients appear to receive durable and long-term benefit. Therefore, predictive biomarkers are needed to identify those likely to respond to immunotherapy [6]. Studies using antibodies against the programmed cell death 1 (PD-1) and programmed death ligand 1 (PD-L1) have shown that PD-L1 tumour proportion score (TPS) could be an indicator of which patients respond best to ICIs, indicating the need for PD-L1 TPS testing in NSCLC patients. Furthermore, it was shown that higher rates of non-synonymous tumour mutations had an association with improved clinical outcomes in patients receiving PD-1/PD-L1 antibodies [6,7].

1.2. Immune checkpoint inhibitor (ICI) therapy for advanced stage NSCLC

Randomized clinical trials of anti-PD-1 therapy showed strong anti-tumour activity in metastatic NSCLC patient cohorts who were already receiving standard of care treatment. The use of nivolumab, a PD-1 inhibitor, was found to improve overall survival (OS) in advanced lung cancer patients with squamous and non-squamous histopathologies when compared to second-line docetaxel [8,9]. An updated analysis of patient survival showed that the median OS for both squamous and non-squamous NSCLC patients treated with nivolumab was greater than that of those treated with docetaxel [10]. As a result, the FDA approved nivolumab as a treatment option for advanced NSCLC [11]. The

* Corresponding author at: Queensland University of Technology, Centre for Genomics and Personalised Health, Cancer and Ageing Research Program, 37 Kent Street, Woolloongabba, Queensland 4102, Australia.
E-mail address: arutha.kulasinghe@qut.edu.au (A. Kulasinghe).

https://doi.org/10.1016/j.lungcan.2021.06.022
Received 20 May 2021; Received in revised form 19 June 2021; Accepted 27 June 2021
Available online 19 July 2021

variation in PD-L1 expression between non-squamous and squamous tumours provided an early indication that PD-L1 expression may not be an ideal predictive biomarker [8,9]. Pembrolizumab, a PD-1 inhibitor, was approved following KEYNOTE-001 discovered a 19.4% objective response rate (ORR) in previously treated NSCLC patients. Furthermore, the KEYNOTE-010, a phase II/III trial for pembrolizumab, showed that patients with a TPS $\geq$ 1% (at least 1% PD-L1 expression) had a better OS when treated with pembrolizumab versus docetaxel. Pembrolizumab was also more effective in patients who had a PD-L1 TPS of at least 50% [12]. The expression of PD-L1 on the surface of tumour-infiltrating immune cells and also tumour cells appeared to be linked to clinical responses. A phase I study of atezolizumab, a PD-L1 inhibitor, revealed that high expression of PD-L1 is linked to clinical responses [13]. Following the POPLAR and OAK trials, atezolizumab was approved for NSCLC patients with metastatic disease who progressed during or after platinum-based chemotherapy [14]. In the POPLAR trial, patients with advanced NSCLC who had previously been treated with atezolizumab or docetaxel had a longer OR in the atezolizumab arm, which was associated with the expression of PD-L1 in immune or tumour cells [15]. In the OAK trial, atezolizumab significantly improved OS in advanced NSCLC patients who had received at least one line of platinum-based chemotherapy. Importantly, in patients with high expression levels of PD-L1 in either immune or tumour cells had the greatest benefit [16]. The ATLANTIC trial (an open-label phase II trial of durvalumab), found an association between ORR and the expression of the PD-L1 on the surface of tumour in advanced NSCLC patients who had previously been treated [17]. Despite this, some patients with low/no PD-L1 expression had an ORR, indicating that PD-L1 may not be an ideal predictive biomarker.

1.3. Immun checkpoint inhibitor (ICI) therapy as first-line treatment in NSCLC

ICIs were investigated in several studies in the first-line setting [18–21]. KEYNOTE-024 compared pembrolizumab to platinum based chemotherapy in untreated advanced NSCLC patients who had PD-L1 TPS of $\geq$50% [18]. Pembrolizumab was shown to improve both median progression-free survival (PFS) and OS to standard of care chemotherapy [19]. Similar results were observed longitudinally, with patients treated with pembrolizumab having a better OS than the chemotherapy treated group [20]. This benefit was seen even after 82 out of 151 patients were transferred from the chemotherapy group to the pembrolizumab treatment arm. It was also found that the use of pembrolizumab, as a single agent, front-line therapy, must be restricted to patients who have a TPS of 50% or higher [21]. These findings were not seen with nivolumab in CheckMate026, a phase III study comparing nivolumab to platinum-based chemotherapy in untreated advanced NSCLC patients who had a PD-L1 TPS of $\geq$1% [22]. Based on the primary efficacy and exploratory analyses, neither patients with a PD-L1 TPS of $\geq$5%, nor those with a PD-L1 TPS $\geq$ 50% had a substantial difference in PFS or OS. Taken together, pembrolizumab remains the only FDA-approved ICI for use as a first-line, single agent.

1.4. PD-L1 expression

PD-L1 immunohistochemistry (IHC) assay was the first companion diagnostic test approved by the FDA for ICIs [23]. This test allows for the estimation of the percentage of tumor cells with an intensity of PD-L1 membranous expression. There are, currently, four FDA-approved assays for measuring PD-L1 in lung cancer: 22C3, 28-8, SP263, and SP142. Several studies on tumour and immune cells have been conducted to compare the sensitivity and reproducibility of these PD-L1 expression assays. Among them, a study sponsored by the National Comprehensive Cancer Network, the Blueprint Project [24] showed that the clone SP142 is less sensitive than the other assays. The FDA has approved the 22C3 pharmDx assay, developed by Agilent Technologies Inc, as a companion diagnostic for pembrolizumab, while others have been approved as complementary [25]. The predictive properties of these assays are limited as it has been demonstrated that clinical benefit is sometimes observed in patients who do not have tumour PD-L1 expression, while some patients, even with high levels of tumour PD-L1 expression, do not benefit from ICIs. As a result, PD-L1 expression status alone is insufficient to predict which patients will benefit from pembrolizumab as a first-line, single-agent treatment for advanced non-squamous NSCLC [26]. A study of 1586 patients with lung adenocarcinoma was conducted to look into PD-L1 expression and targeted next-generation sequencing (using Memorial Sloan Kettering-Integrated Mutation Profiling of Actionable Cancer Targets [MSK-IMPACT]) [27]. The study found that the distribution and predictive value of PD-L1 expression differed between organs, with lymph nodes being enriched for PD-L1 and bones being predominantly PD-L1 negative. Mutations in TP53, MET, and KRAS were linked to PD-L1 high expression, while mutations in EGFR and STK11 were associated with PD-L1 negativity. Overall, it was concluded that the association of PD-L1 expression with the response to ICIs varies between different tissues. In addition, mutations in different genes may have an impact on PD-L1 expression and its predictive value for response to ICIs [27].

1.5. Tumour mutation burden (TMB)

Tumour mutation burden (TMB) is an assessment of the number of somatic mutations found within a tumour sample. The application of this test for immuno-oncology is based on the understanding that an increase in the number of non-synonymous mutations leads to the production of unique tumour neoantigens, which are detected by adaptive immune cells [28,29]. This association has been found in retrospective studies such as Checkmate-026, OAK, and POPLAR, as well as in retrospective non-trial cohorts [7,30–32]. Currently, these findings point to a clinical advantage in terms of ORR or PFS rather than OS. The relationship between mutational burden and response to anti-PD-1/PD-L1 antibodies has been observed in hypermutated tumours, which have been shown to have mutations in DNA repair genes such as MLH1, PMS2, MSH2, and MSH6. The presence of increased $CD8^+$ T cell infiltrates is the most distinguishing feature of these tumours [33,34]. In a study to determine the efficacy of TMB, 1662 advanced cancer patients treated with ICIs and 5371 non-ICI-treated patients were subjected to targeted NGS (MSK-IMPACT). The findings showed a link between a higher somatic TMB (top 20% within each histology) and better OS for patients. This high TMB cutoff for solid cancers were as follows: 5.9 mut/Mb for breast cancer, 10.3 mut/Mb for HNSCC, 13.8 mut/Mb for NSCLC, 30.7 mut/Mb for melanoma, and 52.2 mut/Mb for CRC [35].

1.6. Tumour microenvironment (TME)

Tumours are complex milieu of cells, made up of different types of cells that are interconnected [36]. There are a variety of cell types and factors surrounding the tumour that aid in tumour initiation, growth and dissemination [36]. The TME is formed by cytotoxic or cytoprotective signaling pathways originating in the malignant stroma, endothelial cells, and immune cells [37]. The TME contains a variety of cells and vascularisation involved in tumour growth, either blood vessels or lymphoid vessels, as well as immune infiltrates and extracellular matrix (see Fig. 1) [38]. The interactions of the tumour with its microenvironment influences the tumour growth, invasion, and resistance to treatment [38]. Several factors have been found to influence the TME, including the tumour type, TMB, and immune cell infiltration [39]. A comprehensive and in-depth analysis of TME heterogeneity is critical in determining the best treatment strategy for patients, particularly in patients treated with ICIs, where the degree of immune recognition of the tumour is an important consideration [39]. Bulk tumour analysis, both at the transcriptional and translational levels, cannot reveal a spatially resolved representation of the TME [40]. Recent advances in multiplexed IHC, imaging, and barcoding technologies have paved the

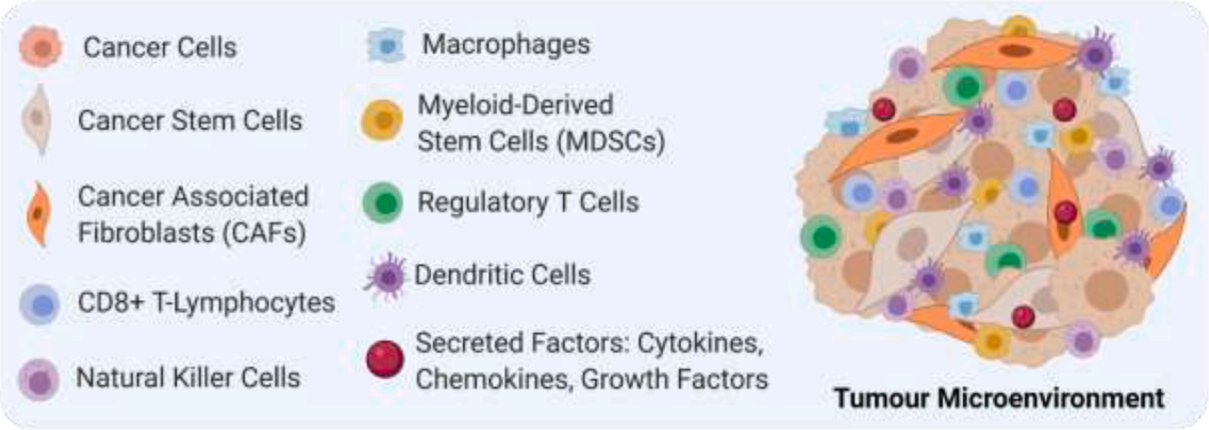

Fig. 1. Composition of the tumour microenvironment. The TME is composed of a complex milieu of multiple cell types encompassing cancer-associated fibroblasts (CAFs), epithelial cells, macrophages, endothelial cells, numerous immune cells and secreted factors, including cytokines, chemokines and growth factors.

way for a better understanding of the TME by addressing the spatial location of cells, and the phenotyping of the TME for composition and function [40]. T cell infiltration into the tumour is thought to provide a degree of immune recognition for effective immunotherapy [41]. As a result, immune contexture (type, density, and location), as well as immune characteristics, such as the phenotypic and functional profile of immune cells, have been used to gain a better understanding of the interactions between immune cells and tumours, potentially leading to the discovery of prognostic biomarkers for anti-PD-1/PD-L1 antibodies [42,43]. While conventional IHC methods allow for tumour spatial profiling, this option is frequently foregone when tumour cells are analyzed using bulk tissue genomic approaches. Furthermore, no characterization of actual cellular proportions, cellular heterogeneity, or deeper spatial distribution exists. The spatial and immunological composition, as well as the cellular status, help to identify micro-niches in the TME [44]. Characterizing the immune context within the TME also paves the way for understanding how immune composition and status (activated/suppressed) influence treatment response. To meet this requirement, simultaneous imaging and tissue sampling are needed to analyze spatially immune cells and tumour tissues.

2. Spatial profiling technologies for lung cancer

Understanding the complex cell types that make up the TME and how they interact sheds light on malignant primary and secondary lung cancers [45,46]. Treatment failure and resistance in primary and secondary lung tumours have revealed that these cells exhibit extensive inter-and intra-tumoural heterogeneity [42,45]. As a result, understanding the molecular relationship between cell types and their morphological and pathological characteristics is critical [45,46]. Since

Table 1
Overview of spatial transcriptomics profiling technologies.

Technology	Approach	Resolution	Sample type	Analyte	Advantages	Disadvantages
MERFISH	• Multiplexed fluorescence imaging	• Cellular	• Fresh-frozen	• RNA	• High resolution • Capable of tracing cell migratory paths • Spatially-resolved RNA • Highly multiplexed	• Limited to 1001 unique mRNAs
10x Visium	• Barcoded mRNA capture spot	• Cellular • Subcellular	• Fresh-frozen	• RNA	• Whole transcriptome	• Barcoded regions contain multiple cells
NanoString DSP	• DNA-barcoding based	• Cellular • Subcellular	• Fresh-frozen • FFPE	• RNA • Protein	• Up to 20,000 mRNA detection • High level of automation	• No image reconstruction • Manually selection of region
NanoString SMI	• in situ chemistry	• Cellular • Subcellular	• Fresh frozen • FFPE	• RNA • Protein	• 3D mapping with subcellular resolution • 1000-plex RNA expression	• Limited profiling area
Ultivue InSituPlex	• DNA-barcoding based	• Cellular • Subcellular	• Fresh frozen • FFPE	• Protein	• Whole-slide imaging and multiplexing • Rapid and automated workflow	• No slide scanner
CODEX	• DNA-barcoding based	• Cellular • Subcellular	• Fresh frozen • FFPE	• Protein	• Removal of sample autofluorescence • Up to 40 protein detection with spatial and single cell resolution	• Time consuming for whole slide analysis • Sample preparation onto coverslip
Imaging Mass Cytometry (IMC)	• Metal-based	• Cellular • Subcellular	• Fresh frozen • FFPE	• Peptides • Protein	• Removal of sample autofluorescence • Molecular analysis with spatial distribution of analytes	• Low throughput • Sample preparation • Data processing and analysis
Hyperion	• Metal-based	• Cellular • Subcellular	• Fresh frozen • FFPE • Liquid biopsies	• Protein	• Highly multiplexed imaging • Capable of quantifying up to 37 protein markers	• Required specialized equipment • Limited in total number of targets • Low sensitivity of probes
MIBIScope	• Metal-based	• Cellular • Subcellular	• Fresh frozen • FFPE	• Protein	• High throughput • Single staining and imaging step • • High sensitivity	• Custom slide required • Time consuming

the late 1990 s, when in-situ sequencing methods to genomic hybridization were developed, the field of spatial biology has grown rapidly, particularly in the last five years [47,48]. From the isolation of targeted regions using laser capture microdissection to multiplex in-situ capturing of proteins/genes, this field has evolved rapidly. Recent studies emphasize the importance of using different transcriptomic/proteomic methods, such as single-cell sequencing, mass cytometry, and multiplex immunofluorescence, to clarify the TME of lung cancers [41,49–51]. While the use of spatial technologies in lung tumours is still in its early stages, emerging studies will help us learn more about these heterogeneous tumours (Table 1) [41,45]. These omics methods have enabled the visualization of molecularly defined cell types as well as the simultaneous identification of RNA and protein markers, opening up new avenues for lung cancer characterization [41,45]. Recently, spatially resolved transcriptomics was named the method of the year by Nature Methods [52]. As this technology is rapidly gaining traction in oncology research, recent studies in the literature provide a general explanation of how the various technologies encode spatial information [47,53].

2.1. Multiplexed error-robust fluorescence in situ hybridization (MERFISH)

Multiplexed error-robust fluorescence in situ hybridization (MERFISH) is a technique for imaging individual RNA molecules at the single cell level. Individual RNA species are first assigned to error-robust barcodes, then labeled with oligonucleotides, each of which represents a barcode, and finally, sequential single-molecule FISH imaging is used to read out these barcodes [54–56]. Not only does it provide quantitative measurement of RNA expression, but it also determines the spatial localization of individual RNA molecules in freshly frozen tissues, making it highly accurate and with a high detection efficiency [54,57]. These properties have led to new insights into biological processes, including cell polarization, cell migration, cell fate determination during cell division, and local translation [58]. As a result, using this technology, it is possible to map, count, and image thousands of RNA species in single cells at the same time, as well as delineate regulatory networks and identify cell types in situ. This technology, however, is currently limited to 1001 mRNA molecules [54].

2.2. 10x Genomics Visium spatial gene expression

Visium is a spatial transcriptomic technology that can profile tissues using a lawn of capture probes [39]. Visium can be applied to freshly frozen samples using thousands of barcoded mRNA capture spots, thus, it can quantify gene expression with whole-transcriptome resolution [59]. In addition to identifying distinct cell groups, the technology is also able to demonstrate a relationship between cell function, phenotype, and location in TME while preserving the spatial context of tissues [39,60,61]. Visium, therefore, has specific clinical applications such as studying tumour heterogeneity and tissue morphology, discovering novel biomarkers, and identifying responses to therapeutic interventions [59]. The first step involves the carefully placement of the tissue specimen over the capture area of the slide [62]. Following tissue fixation and permeabilization, RNA is released and binds to capture probes, resulting in the capture of gene expression data [62]. Following this, the cDNA is synthesized, and the bound genetic data is collected and spatially analyzed. This technology has a few limitations, such as the need for fresh tissues and the current need for an optimized workflow. Each of the slides has four capture areas, each containing 5,000 barcode spots, each with millions of probes [63]. As a result, creating transcription profiling of thousands of individual locations is simple; however, the barcoded regions may contain multiple cells [63]. FFPE and single cell compatibility is expected with their upcoming Visium HD technology.

2.3. Nanostring GeoMx^{TM} Digital Spatial Profiler (DSP)

Nanostring GeoMx^{TM} Digital Spatial Profiler (DSP) is a non-destructive technique for profiling in-depth RNA/protein expression [64]. The DSP platform, which employs oligonucleotide detection technology, allows for multiplexed quantification of RNA and proteins with spatial resolution down to a few cells from fresh frozen or fixed tissue specimens [65]. Following the preparation of the tissue, samples are incubated with visualization markers (e.g., pan-cytokeratin, CD8, and CD3) and conjugated with oligonucleotide tags [66]. Following that, the tissue architecture is delineated using a set of user-defined Regions of interest (ROIs). Finally, the oligonucleotide tags are released from discrete regions by ultraviolet (UV) exposure and subjected to counting/sequencing to generate a spatially resolved profile of the analyte abundance [66]. The DSP provides several advantages, such as user-defined ROI analysis and multispectral imaging [67]. By using a UV-photocleavable signal, DSP can also eliminate the need for chemical stripping, which is a disadvantage of other multi-color IHC techniques. The DSP platform is regarded as a valuable addition to current single-staining IHC methods in clinical diagnostics, as it enables high-plex and high-throughput RNA/protein spatial profiling [67,68]. In the study by Monkman et al. in NSCLC patients, they found that the TME was significantly enriched in CD3, CD4, CD27, CD45, CD45RO, CD68, CD163, and VISTA when compared to the tumour. Normal adjacent tissues, on the other hand, were found to be enriched in fibronectin, CD34, IDO1, ARG1, LAG3, and PTEN relative to the TME. Furthermore, the study found a link between improved OS and the presence of cells expressing CD3, CD34, and ICOS in tumour compartments [45]. Moreover, Zugazagoitia et al., identified predictive biomarkers of response to ICIs in NSCLC. The study applied the DSP technology to samples from immunotherapy-treated NSCLC patients and quantified multiple immune parameters in tissue compartments, including tumour, leucocytes, macrophages, and non-immune stroma. They discovered 18 markers related to outcomes in the spatial context, of which CD4 and CD56 measured in the leucocytes, and CD56 measured in the stroma were the predictive markers associated with clinical outcomes, including PFS and OS [68]. One of the challenges is achieving single-cell resolution compatibility, which is currently being developed with the Spatial Molecular Imager (SMI).

2.4. Nanostring spatial molecular Imager (SMI)

The Nanostring SMI is an integrated system that includes mature cyclic in situ hybridization chemistry, a high-resolution imaging readout instrument, and interactive data analysis and visualization software. NanoString's SMI technology is capable of analyzing hundreds to thousands of RNAs or proteins directly from single cells with subcellular resolution within morphologically intact tissue samples. The SMI combines the power of high-plex profiling with high-resolution imaging, allowing researchers to quantify and visualize targeted protein and gene expression in tissue sections. Sample preparation consists of standard in situ hybridization processing steps that allow the use of pathology lab-standard glass slides, as well as the absence of cDNA synthesis or amplification. The SMI relies on highly multiplexed in-situ hybridization chemistry as well as direct single molecule imaging and counting. The detection of RNA or protein targets in individual cells is accomplished through the hybridization of targets with specific probes or antibodies labeled with a unique barcode system. The barcode readout is then performed using cyclic rounds of fluorescently labeled reporter probe imaging. In cells, each RNA or protein appears as a single spot that can be digitally quantified by counting the number of imaged spots. The SMI technology uses no reverse transcription, amplification, or enzymes, resulting in high detection efficiency and unbiased quantification. Taken together, pre-designed panels up to 1000-plex, accurate detection of low copy number genes, 3-Dimensional mapping with subcellular resolution, and quantifying single-cell biomarkers with spatial context are

some of the distinguishing features of the SMI technology (see Fig. 2).

2.5. Ultivue InSituPlex

Using InSituPlex DNA-barcoding and antibody staining technologies, the Ultivue enables spatial profiling of tissue biomarkers as well as whole-slide multiplexing of cell phenotyping [69]. The platform implements a delicate staining process to preserve the integrity of the tissue sample [70]. InSituPlex technology identifies various markers in single cells across a wide range of cellular components, including the nucleus, cytoplasm, and plasma membrane [71]. These features lead to more accurate and in-depth immunophenotyping of tissues through positive detection of markers [71]. Using the barcode linear amplification technique, this technology can monitor different marker-to-marker and cell-to-cell expression levels, as well as increase the number of hybridization sites for imaging [70]. In addition to high-performance tissue multiplexing, this platform is able to quantify biomarker co-localization and co-expression [72]. To visualize tumour samples, they must be dewaxed and retrieved, followed by three steps of staining, amplification, and detection [73]. Samples are incubated with a blend of barcoded antibodies, each with a unique DNA sequence. Following the simultaneous amplification of the targets, they bind to complementary fluorescent DNA probes and are then prepared for imaging [73]. The Ultivue platform is distinguished by the fact that each step of retrieval, staining, amplification, and detection is performed only once, and the entire process takes roughly 5.5 h, though the absence of a preexisting slide scanner may impede the progress of the analysis [69]. Humphries et al. used Ultivue to see if digital image analysis (DIA) and multiplexed immunofluorescence could improve the accuracy of PD-L1 diagnostic testing. In the study, they discovered that using DIA for PD-L1 expression analysis had a significant concordance with manual assessment with an sensitivity of 86.8 % and specificity was 91.4%. Furthermore, the study found that PD-L1+/CD68+ macrophages could be easily detected within PD-L1+/cytokeratin+ or PD-L1-/cytokeratin+ tumour nests using multiplexing [72].

2.6. CO-Detection by antibody indexing (CODEX)

CO-Detection by antibody indexing (CODEX) is a multiplex fluorescence microscopy platform that analyzes 40 target molecules in a tissue section using DNA-conjugated antibodies [74]. The CODEX technology speeds up the process by using a single initial staining step and multiple imaging steps after that, as well as removing the antibody conjugated barcodes. It also prevents tissue degradation, which is a disadvantage of other cyclic immunofluorescence (CycIF) approaches [75]. DNA-conjugated antibodies are visualized using complementary fluorescent DNA probes, which are then accompanied by imaging, probe stripping, washing, and re-rendering [75]. This platform is used to identify individual cells within a tissue, as well as to discover new cell types and cell–cell interactions. As a result, CODEX offers multiplexed marker detection at the level of a single cell unit in the spatial context, allowing for a more in-depth examination of the TME [74].

2.7. Imaging mass cytometry (IMC)

Imaging Mass Cytometry (IMC) is a mass cytometry approach employing metal-conjugated antibodies [76]. IMC can measure the expression of up to 50 markers with subcellular spatial resolution. IMC has been demonstrated in frozen as well as FFPE tissue sections [76]. Labeling is first performed on tissue sections with several antibodies

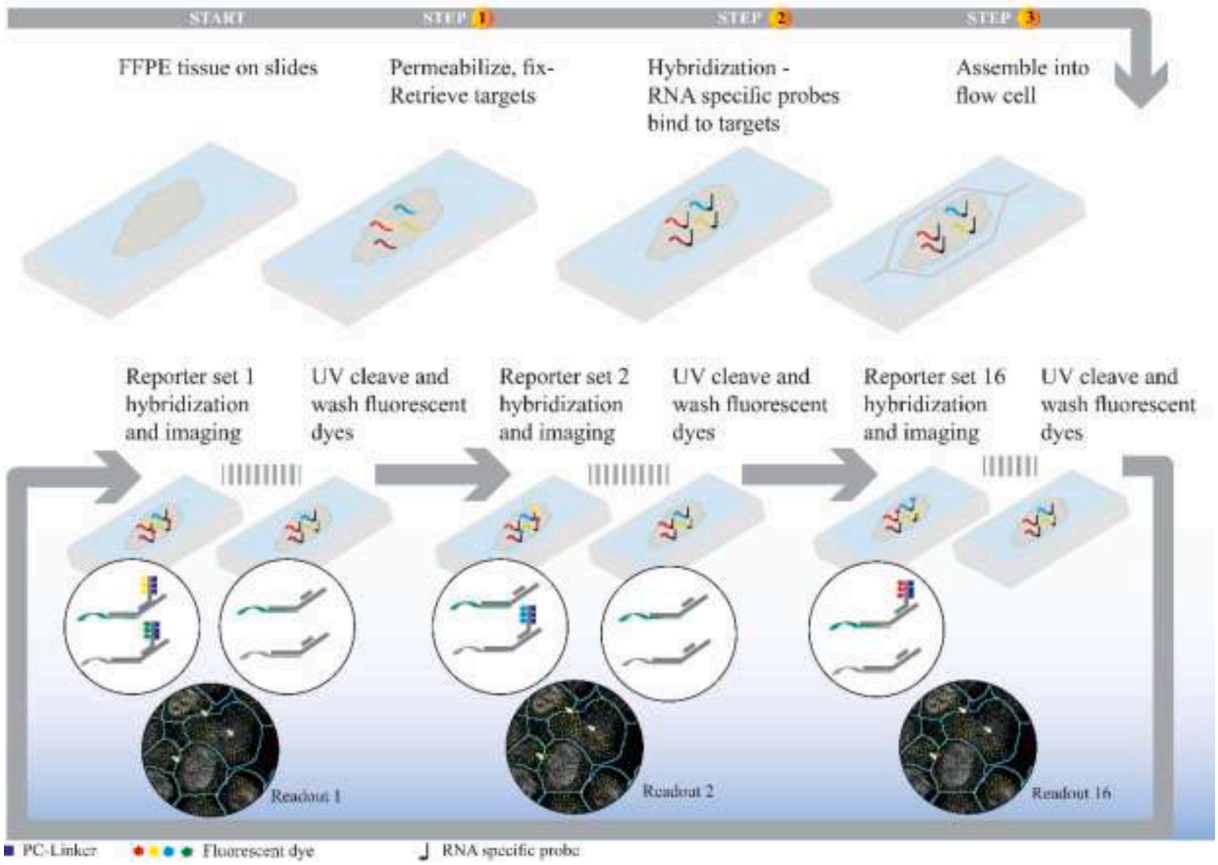

Fig. 2. Spatial Molecular Imager workflow. Hyb and Seq chemistry with cyclic imaging is used to gain single cell, and sub-cellular resolution from 100 to 1000 genes. Each fluorescent signal/transcript is tracked in 3D (x, y and z coordinates) assigned to individual cells and subcellular components. Image adapted from https://www.nanostring.com/products/spatial-molecular-imaging/spatial-molecular-imaging-technology-overview/.

attached to stable isotopes [77]. These sections are then cut with a laser system to produce segments with 1 μm in diameter [78]. Followed atomization and ionization, the metal-isotope content of each segment is quantified using a time-of-flight mass analyzer. Pseudo-colored and spatially assigned images are generated based on the isotope abundance of each spot [77]. IMC is distinct from traditional immunofluorescence (IF) methods in that it is free of autofluorescence, spectral overlap, and signal fading [79]. By generating spatial information, IMC provides a more precise view of cell subsets and cell–cell interactions. In addition, IMC can be used to visualize proteins in various cell compartments such as the nucleus, cytoplasm, and membrane, potentially leading to the discovery of new biomarkers [79]. However, this technology has some limitations, including the time-consuming sample preparation and data processing/analysis, as well as the high cost of antibodies.

2.8. Hyperion imaging system

Hyperion Imaging System is an antibody-directed IMC platform with highly multiplexed imaging capabilities [80]. Using standard staining methods, this system is able to identify metal-tagged antibodies bound to proteins in biological samples [80]. The platform can also quantify up to 37 protein markers in biological samples, such as fixed tissue sections or liquid biopsies at the same time [81]. The platform combines cellular profiling with spatial context, allowing for subpopulation profiling and the investigation of neighboring cell interactions within a tissue [81]. Hyperion is a system that combines laser ablation technology with time-of-flight (TOF) mass cytometry of the resulting plume [82]. A precisely directed laser beam is used to collect protein markers impregnated with metal-tagged Maxpar antibodies [82]. These metal tags are then directed for detection using CyTOF technology [83]. The sample is first ablated and aerosolized [83]. Through the argon and helium flow, the resulting aerosol plume is transferred to the Helios inductively coupled plasma (ICP) torch [83]. The slide is placed on the ablation chamber's base, and the image from the slide is captured by the camera [84]. Through the optical components of the chamber, the system emits a laser beam [84]. The laser beam focuses on a 1 μm spot and ablates metal-tagged antibody-stained proteins, generating aerosol plumes [85]. The plume is the material that results from the laser beam to the sample slide. These plumes are guided to the Helios ICP Torch in order to be vaporized, atomized, and ionized in the plasma [85]. Finally, the TOF mass analyzer measures the quantity of each isotope in each plume, which corresponds to a single laser shot, from the sample using mass differences rather than wavelength differences [80].

2.9. Multiplexed ion beam imaging (MIBI) technology

Multiplexed ion beam imaging (MIBI) Technology is developed on the basis of secondary ion mass spectrometry (SIMS) [86]. SIMS works by rastering a primary ion beam across the surface of a sample and releasing the reporting ions, which are then recorded pixel by pixel using TOF detection. In comparison to a laser, an ion beam allows for resolution adjustment over a wide range, such as 280 nm to 1 μm in the case of the MIBIScope [86]. Once released, the reporter ions travel at supersonic speeds from the sample to the detector, resulting in rapid acquisition and exceptional sensitivity [87]. This technology is therefore capable of quantifying protein expression, phenotyping immune infiltrates, and profiling tissue architecture. MIBI can also be applied to all common sample types, for example, FFPE and fresh-frozen tissue [87]. Using a standard IHC staining protocol, a tissue sample is stained with metal-tagged antibodies [88]. Low-resolution survey scans can also be obtained before high-resolution imaging [88]. During imaging, the sample is not destroyed and can be retained for further studies or analysis. MIBI generates TIFF images, which can be quickly and easily viewed in MIBItracker or exported for further analysis in other software. More than 40 markers can thus be visualized in a single staining and imaging step. The MIBIscope is currently validated by the National Cancer Institute (NCI) as the only multiplex imaging assay for clinical trials [89].

3. Conclusion

To develop more effective treatments for NSCLC, a better understanding of the complexities associated with tumour heterogeneity in primary and metastatic lung cancers is required. Advances in spatial profiling technology have empowered the next generation of digital pathology, revealing new insights into tumour heterogeneity, resistance mechanisms, and potential biomarkers that may predict treatment outcomes. Such advancements have resulted in the digitization of tumour assessment, from scoring to quantifiable cell counts, cellular expression data with spatial resolution, allowing for a deeper understanding of the cellular players, immune status, and cell activation within the TME. Spatial profiling technologies enable comprehensive analyses of tissue expression, morphology, and protein or gene expression, as well as previously unattainable biological insights into tumours, allowing for a better understanding of tumour-immune cell interactions. Whilst most current technologies can resolve down to a few cells, we anticipate single cell and sub-cellular resolution being developed. We envisage that the findings from these complimentary technologies may lead to the development of predictive cellular phenotypes and signatures associated with response to immunotherapy in NSCLC.

Declaration of Competing Interest

The authors declare that they have no known competing financial interests or personal relationships that could have appeared to influence the work reported in this paper.

Acknowledgement

AK is supported by an NHMRC Fellowship (APP1157741) and Cure Cancer (APP1182179). KOB is supported by the Princess Alexandra Hospital Foundation (PARF).

References

[1] R.L. Siegel, K.D. Miller, A. Jemal, Cancer statistics, 2019. CA: a cancer journal for clinicians, 2019. 69(1): p. 7-34.
[2] N. Howlader, et al., SEER Cancer Statistics Review, 1975-2016. National Cancer Institute. Bethesda, MD, based on November 2018 SEER data submission, posted to the SEER web site, April 2019. 2020.
[3] W. Pao, N. Girard, New driver mutations in non-small-cell lung cancer, Lancet Oncol. 12 (2) (2011) 175–180.
[4] F.R. Hirsch, et al., Lung cancer: current therapies and new targeted treatments, The Lancet 389 (10066) (2017) 299–311.
[5] Q.-G. Zhu, et al., Driver genes in non-small cell lung cancer: characteristics, detection methods, and targeted therapies, Oncotarget 8 (34) (2017) 57680.
[6] K.C. Arbour, G.J. Riely, Systemic therapy for locally advanced and metastatic non–small cell lung cancer: a review, JAMA 322 (8) (2019) 764–774.
[7] N.A. Rizvi, et al., Mutational landscape determines sensitivity to PD-1 blockade in non–small cell lung cancer, Science 348 (6230) (2015) 124–128.
[8] J. Brahmer, et al., Nivolumab versus docetaxel in advanced squamous-cell non–small-cell lung cancer, N. Engl. J. Med. 373 (2) (2015) 123–135.
[9] H. Borghaei, et al., Nivolumab versus docetaxel in advanced nonsquamous non–small-cell lung cancer, N. Engl. J. Med. 373 (17) (2015) 1627–1639.
[10] L. Horn, et al., Nivolumab versus docetaxel in previously treated patients with advanced non–small-cell lung cancer: two-year outcomes from two randomized, open-label, phase III trials (CheckMate 017 and CheckMate 057), J. Clin. Oncol. 35 (35) (2017) 3924.
[11] D. Kazandjian, et al., FDA approval summary: nivolumab for the treatment of metastatic non-small cell lung cancer with progression on or after platinum-based chemotherapy, Oncologist 21 (5) (2016) 634.
[12] R.S. Herbst, et al., Pembrolizumab versus docetaxel for previously treated, PD-L1-positive, advanced non-small-cell lung cancer (KEYNOTE-010): a randomised controlled trial, The Lancet 387 (10027) (2016) 1540–1550.
[13] R.S. Herbst, et al., Predictive correlates of response to the anti-PD-L1 antibody MPDL3280A in cancer patients, Nature 515 (7528) (2014) 563–567.
[14] C. Weinstock, et al., US Food and Drug Administration approval summary: atezolizumab for metastatic non–small cell lung cancer, Clin. Cancer Res. 23 (16) (2017) 4534–4539.

[15] L. Fehrenbacher, et al., Atezolizumab versus docetaxel for patients with previously treated non-small-cell lung cancer (POPLAR): a multicentre, open-label, phase 2 randomised controlled trial, The Lancet 387 (10030) (2016) 1837–1846.
[16] A. Rittmeyer, et al., Atezolizumab versus docetaxel in patients with previously treated non-small-cell lung cancer (OAK): a phase 3, open-label, multicentre randomised controlled trial, The Lancet 389 (10066) (2017) 255–265.
[17] M.C. Garassino, et al., Durvalumab as third-line or later treatment for advanced non-small-cell lung cancer (ATLANTIC): an open-label, single-arm, phase 2 study, Lancet Oncol. 19 (4) (2018) 521–536.
[18] M. Reck, et al., Pembrolizumab versus chemotherapy for PD-L1–positive non–small-cell lung cancer, N Engl J Med 375 (2016) 1823–1833.
[19] L. Pai-Scherf, et al., FDA approval summary: pembrolizumab for treatment of metastatic non-small cell lung cancer: first-line therapy and beyond, Oncologist 22 (11) (2017) 1392.
[20] J. Brahmer, et al., OA 17.06 updated analysis of KEYNOTE-024: Pembrolizumab vs platinum-based chemotherapy for advanced NSCLC with PD-L1 TPS≥ 50%, J. Thoracic Oncol. 12 (11) (2017) S1793–S1794.
[21] G. Lopes, et al., Pembrolizumab (pembro) versus platinum-based chemotherapy (chemo) as first-line therapy for advanced/metastatic NSCLC with a PD-L1 tumor proportion score (TPS)≥ 1%: open-label, phase 3 KEYNOTE-042 study. 2018, American Society of Clinical Oncology.
[22] D.P. Carbone, et al., First-line nivolumab in stage IV or recurrent non–small-cell lung cancer, N. Engl. J. Med. 376 (25) (2017) 2415–2426.
[23] B.C. Calhoun, L.C. Collins, Predictive markers in breast cancer: An update on ER and HER2 testing and reporting. Seminars in diagnostic pathology, Elsevier, 2015.
[24] R. Büttner, et al., Programmed death-ligand 1 immunohistochemistry testing: a review of analytical assays and clinical implementation in non–small-cell lung cancer, J. Clin. Oncol. 35 (34) (2017) 3867–3876.
[25] M. Hersom, J.T. Jørgensen, Companion and complementary diagnostics–focus on PD-L1 expression assays for PD-1/PD-L1 checkpoint inhibitors in non–small cell lung Cancer, Ther. Drug Monit. 40 (1) (2018) 9–16.
[26] D.B. Doroshow, et al., Immunotherapy in non–small cell lung cancer: facts and hopes, Clin. Cancer Res. 25 (15) (2019) 4592–4602.
[27] A.J. Schoenfeld, et al., Clinical and molecular correlates of PD-L1 expression in patients with lung adenocarcinomas, Ann. Oncol. 31 (5) (2020) 599–608.
[28] T.N. Schumacher, R.D. Schreiber, Neoantigens in cancer immunotherapy, Science 348 (6230) (2015) 69–74.
[29] T. Davoli, et al., Tumor aneuploidy correlates with markers of immune evasion and with reduced response to immunotherapy, Science 355 (6322) (2017).
[30] S. Peters, et al., Abstract CT082: Impact of tumor mutation burden on the efficacy of first-line nivolumab in stage iv or recurrent non-small cell lung cancer: An exploratory analysis of CheckMate 026. 2017, AACR.
[31] D.R. Gandara, et al., Blood-based tumor mutational burden as a predictor of clinical benefit in non-small-cell lung cancer patients treated with atezolizumab, Nat. Med. 24 (9) (2018) 1441–1448.
[32] S. Gettinger, et al., A dormant TIL phenotype defines non-small cell lung carcinomas sensitive to immune checkpoint blockers, Nat. Commun. 9 (1) (2018) 1–15.
[33] R. Dolcetti, et al., High prevalence of activated intraepithelial cytotoxic T lymphocytes and increased neoplastic cell apoptosis in colorectal carcinomas with microsatellite instability, Am. J. Pathol. 154 (6) (1999) 1805–1813.
[34] T.C. Smyrk, et al., Tumor-infiltrating lymphocytes are a marker for microsatellite instability in colorectal carcinoma, Cancer 91 (12) (2001) 2417–2422.
[35] R.M. Samstein, et al., Tumor mutational load predicts survival after immunotherapy across multiple cancer types, Nat. Genet. 51 (2) (2019) 202–206.
[36] S. Herath, et al., Circulating tumor cell clusters: Insights into tumour dissemination and metastasis, Expert Rev. Mol. Diagn. 20 (11) (2020) 1139–1147.
[37] D. Hanahan, L.M. Coussens, Accessories to the crime: functions of cells recruited to the tumor microenvironment, Cancer Cell 21 (3) (2012) 309–322.
[38] M. Binnewies, et al., Understanding the tumor immune microenvironment (TIME) for effective therapy, Nat. Med. 24 (5) (2018) 541–550.
[39] B. He, et al., Integrating spatial gene expression and breast tumour morphology via deep learning, Nat. Biomed. Eng. (2020) 1–8.
[40] P.L. Ståhl, et al., Visualization and analysis of gene expression in tissue sections by spatial transcriptomics, Science 353 (6294) (2016) 78–82.
[41] X. Guo, et al., Global characterization of T cells in non-small-cell lung cancer by single-cell sequencing, Nat. Med. 24 (7) (2018) 978–985.
[42] T.J. Welsh, et al., Macrophage and mast-cell invasion of tumor cell islets confers a marked survival advantage in non–small-cell lung cancer, J. Clin. Oncol. 23 (35) (2005) 8959–8967.
[43] N.A. Giraldo, et al., Multidimensional, quantitative assessment of PD-1/PD-L1 expression in patients with Merkel cell carcinoma and association with response to pembrolizumab, J. ImmunoTher. Cancer 6 (1) (2018) 1–11.
[44] J.M. Beechem, High-Plex Spatially Resolved RNA and protein detection using digital spatial profiling: a technology designed for immuno-oncology biomarker discovery and translational research, in: Biomarkers for Immunotherapy of Cancer, Springer, 2020, pp. 563–583.
[45] J. Monkman, et al., High-Plex and High-throughput Digital Spatial Profiling of non-small-cell lung cancer (NSCLC), Cancers 12 (12) (2020) 3551.
[46] H. Sadeghi Rad, et al., Understanding the tumor microenvironment for effective immunotherapy, Med. Res. Rev. (2020).
[47] M. Asp, J. Bergenstråhle, J. Lundeberg, Spatially resolved transcriptomes—next generation tools for tissue exploration, BioEssays 42 (10) (2020) 1900221.
[48] P. Kalita-de Croft, et al., Spatial profiling technologies and applications for brain cancers, Expert Rev. Mol. Diagnostics (2021).
[49] A. Kulasinghe, et al., The use of three-dimensional dna fluorescent in situ hybridization (3D DNA FISH) for the detection of anaplastic lymphoma kinase (ALK) in non-small cell lung cancer (NSCLC) circulating tumor cells, Cells 9 (6) (2020) 1465.
[50] D.S. O'Callaghan, et al., Tumour islet Foxp3+ T-cell infiltration predicts poor outcome in nonsmall cell lung cancer, Eur. Respir. J. 46 (6) (2015) 1762–1772.
[51] D.E. Swinson, et al., Carbonic anhydrase IX expression, a novel surrogate marker of tumor hypoxia, is associated with a poor prognosis in non–small-cell lung cancer, J. Clin. Oncol. 21 (3) (2003) 473–482.
[52] from Xiaowei, A.C., Method of the Year 2020: spatially resolved transcriptomics.
[53] S. Maniatis, J. Petrescu, H. Phatnani, Spatially resolved transcriptomics and its applications in cancer, Curr. Opin. Genet. Dev. 66 (2021) 70–77.
[54] K.H. Chen, et al., Spatially resolved, highly multiplexed RNA profiling in single cells, Science 348 (6233) (2015).
[55] J.R. Moffitt, et al., High-performance multiplexed fluorescence in situ hybridization in culture and tissue with matrix imprinting and clearing, Proc. Natl. Acad. Sci. 113 (50) (2016) 14456–14461.
[56] J.R. Moffitt, et al., Molecular, spatial, and functional single-cell profiling of the hypothalamic preoptic region, Science 362 (6416) (2018).
[57] C. Xia, et al., Multiplexed detection of RNA using MERFISH and branched DNA amplification, Sci. Rep. 9 (1) (2019) 1–13.
[58] A.R. Buxbaum, G. Haimovich, R.H. Singer, In the right place at the right time: visualizing and understanding mRNA localization, Nat. Rev. Mol. Cell Biol. 16 (2) (2015) 95–109.
[59] Y. Wang, S. Ma, W.L. Ruzzo, Spatial modeling of prostate cancer metabolic gene expression reveals extensive heterogeneity and selective vulnerabilities, Sci. Rep. 10 (1) (2020) 1–14.
[60] A. Andersson, et al., Single-cell and spatial transcriptomics enables probabilistic inference of cell type topography, Commun. Biol. 3 (1) (2020) 1–8.
[61] D.T. Pham, et al., stLearn: integrating spatial location, tissue morphology and gene expression to find cell types, cell-cell interactions and spatial trajectories within undissociated tissues. bioRxiv, 2020.
[62] K.E. Maynard, et al., Transcriptome-scale spatial gene expression in the human dorsolateral prefrontal cortex. bioRxiv, 2020.
[63] S. Maniatis, et al., Spatiotemporal dynamics of molecular pathology in amyotrophic lateral sclerosis, Science 364 (6435) (2019) 89–93.
[64] M.I. Toki, et al., Validation of novel high-plex protein spatial profiling quantitation based on NanoString's Digital Spatial Profiling (DSP) technology with quantitative fluorescence (QIF). 2017, AACR.
[65] H. Sadeghi Rad, et al., The evolving landscape of predictive biomarkers in immuno-oncology with a focus on spatial technologies, Clin. Transl. Immunol. 9 (11) (2020), e1215.
[66] T.M. Van, C.U. Blank, A user's perspective on GeoMxTM digital spatial profiling, Immuno-Oncol. Technol. 1 (2019) 11–18.
[67] A. Kulasinghe, et al., Highly multiplexed digital spatial profiling of the tumour microenvironment of head and neck squamous cell carcinoma patients, Front. Oncol. 10 (2020) 3118.
[68] J. Zugazagoitia, et al., Biomarkers associated with beneficial PD-1 checkpoint blockade in non-small cell lung cancer (NSCLC) identified using high-plex digital spatial profiling, Clin Cancer Res 26 (16) (2020) 4360–4368.
[69] T. Navas, et al., A multiplex immunofluorescence assay to assess immune checkpoint inhibitor-targeted CD8 activation and tumor colocalization in FFPE tissues, J. Clin. Oncol. 37 (15) (2019) 2629.
[70] S. O'Neil, et al. Use of Ultivue InSituPlex (R) multiplex immunofluorescence to localize and quantify regulatory T lymphocytes in formalin-fixed paraffin-embedded human tissue sections. in JOURNAL FOR IMMUNOTHERAPY OF CANCER. 2019. BMC CAMPUS, 4 CRINAN ST, LONDON N1 9XW, ENGLAND.
[71] A.H. Sastre, et al., Looking beyond the assay: Comparison of multiplex chromogenic and fluorescent immunohistochemistry for standardized immune oncology profiling in non-small cell lung carcinoma patients. in JOURNAL FOR IMMUNOTHERAPY OF CANCER. 2019. BMC CAMPUS, 4 CRINAN ST, LONDON N1 9XW, ENGLAND.
[72] M.P. Humphries, et al., Improving the diagnostic accuracy of the PD-L1 test with image analysis and multiplex hybridization, Cancers (Basel) 12 (5) (2020).
[73] D. Blanco-Melo, et al., Imbalanced host response to SARS-CoV-2 drives development of COVID-19, Cell 181 (5) (2020) 1036–1045.e9.
[74] C. Schuerch, et al., Dynamics of the bone marrow microenvironment during leukemic progression revealed by codex hyper-parameter tissue imaging. Blood, 2018. 132(Supplement 1): p. 935-935.
[75] A. Rahman, et al., Advances in tissue-based imaging: impact on oncology research and clinical practice, Expert Rev. Mol. Diagnostics 20 (10) (2020) 1027–1037.
[76] H. Baharlou, et al., Mass cytometry imaging for the study of human diseases—applications and data analysis strategies, Front. Immunol. 10 (2019) 2657.
[77] A. Mavropoulos, et al., Equivalence of imaging mass cytometry and immunofluorescence on FFPE tissue sections. White paper.
[78] H. Barber, et al., Advanced molecular characterization using Digital Spatial Profiling Technology on immuno-oncology targets in methylated compared with unmethylated IDH-wildtype glioblastoma, Neuro-Oncology 21 (Supplement_4) (2019) p. iv8-iv8.
[79] Q. Chang, et al., Imaging mass cytometry, Cytometry part A 91 (2) (2017) 160–169.
[80] S. Xie, et al., Hyperion imaging system reveals heterogeneous tumor microenvironment of oral squamous cell carcinoma patients at T1N0M0 stage, Ann. Transl. Med. 8 (22) (2020).

[81] J. Bassan, M. Nitz, Methods for analyzing tellurium imaging mass cytometry data, PLoS ONE 14 (9) (2019), e0221714.
[82] S. Chevrier, et al., Compensation of signal spillover in suspension and imaging mass cytometry. Cell Systems, 2018. 6(5): p. 612-620. e5.
[83] E. Gerdtsson, et al., Multiplex protein detection on circulating tumor cells from liquid biopsies using imaging mass cytometry, Convergent Sci. Phys. Oncol. 4 (1) (2018), 015002.
[84] Y. Zhang, et al., Inflammatory response cells during acute respiratory distress syndrome in patients with coronavirus disease 2019 (COVID-19), Ann. Intern. Med. 173 (5) (2020) 402–404.
[85] N. Guo, et al., A 34-marker panel for imaging mass cytometric analysis of human snap-frozen tissue, Front. Immunol. 11 (2020) 1466.
[86] J. Ptacek, et al., Multiplexed ion beam imaging (MIBI) for characterization of the tumor microenvironment across tumor types, Lab. Invest. (2020) 1–13.
[87] J. Ptacek, et al., 48 Advances in multiplexed ion beam imaging (MIBI) for immune profiling of the tumor microenvironment. 2020, BMJ Specialist Journals.
[88] S. Rost, et al., Multiplexed ion beam imaging analysis for quantitation of protein expresssion in cancer tissue sections, Lab. Invest. 97 (8) (2017) 992–1003.
[89] L. Keren, et al., A structured tumor-immune microenvironment in triple negative breast cancer revealed by multiplexed ion beam imaging. Cell, 2018. 174(6): p. 1373-1387. e19.